Optical and Quantum Electronics 17 *(1985) 53–68*

S_n-state lifetime determination of dyes

F. GRAF, A. PENZKOFER
Naturwissenschaftliche Fakultät – Physik, Universität Regensburg, 8400 Regensburg, FRG

Received 9 July 1984

The S_n-state lifetime is determined from two-step excited S_n–S_0 fluorescence yield measurements with picosecond light pulses. The theoretical analysis includes single pulse and double pulse consecutive excitation and takes into account the anisotropy of excitation and emission. Experimental results of the single pulse two-step excitation technique are presented for the S_4-state lifetimes of the three mode-locking dyes 5, 9740 and 9860 for Nd-glass lasers.

1. Introduction

The lifetimes of higher excited singlet states S_n ($n \geqslant 2$) of dye solutions are generally in the subpicosecond range [1–10]. S_2-state lifetimes in the picosecond [11–18] and nanosecond regions [19–21] have been found in only a few dye molecules. The conventional technique of lifetime determination by fluorescence quantum yield measurement after single-step dye excitation is limited to quantum yields $q_F = \tau_F/\tau_{rad} \gtrsim 10^{-3}$ (fluorescence lifetime $\tau_F \gtrsim 10$ ps; τ_{rad}, radiative lifetime). It is frequently used for S_1-state lifetime measurement [22–27]. The measurement of small quantum yields by single-step excitation is limited by the fluorescence of impurities or photoproducts. Also, Raman scattering of the solvent may cause disturbance.

In two-step excitation from S_0 to S_1 and from S_1 to S_n the problems of impurity fluorescence and Raman scattering are avoided. Two-step excitation with a single laser pulse (single frequency) [3, 28–38] and with two laser pulses of different frequency [1, 4, 7, 10, 33, 34] have been performed. S_n–S_0 fluorescence spectra have been reported.

The determination of S_n-state lifetimes by two-step excited fluorescence quantum yield measurement is only scantily reported [1, 4, 7, 10] because of the difficulty of determining the S_n-state population.

In this paper we derive expressions for the fluorescence signal by two-step pulse or double pulse excitation that allow determination of the S_n-state lifetime. The influence of the anisotropy of light absorption and emission by the electric dipole interaction is analysed. Possible disturbances by two-photon absorption of impurities are discussed. In the experiments the S_4-state lifetimes of three mode-locking dyes 5, 9740 and 9860, for Nd-glass lasers, are determined. The two-step single pulse excitation technique is applied with picosecond light pulses from an Nd-glass laser.

2. Theory

In the experiments the S_n–S_0 fluorescence energy W_F normalized to the input pulse energy W_L will be measured and compared with the S_1–S_0 fluorescence signal of a reference dye of known quantum efficiency. This comparison avoids absolute quantum yield measurements.

In Fig. 1 relevant level schemes are depicted for consecutive single pulse excitation (a), consecutive double pulse excitation (b) and reference dye excitation (c). In each case the fluorescence from an upper level $|u\rangle$ in S_n or S_1 (reference) to a lower level in S_0 is observed. The geometrical arrangement is shown in Fig. 2. The excitation pulses propagate along the y-axis and are vertically polarized (along the z-axis). The fluorescence is observed perpendicular to the pump pulse propagation in the x-direction. The

0306–8919/85 \$03.00 + .12

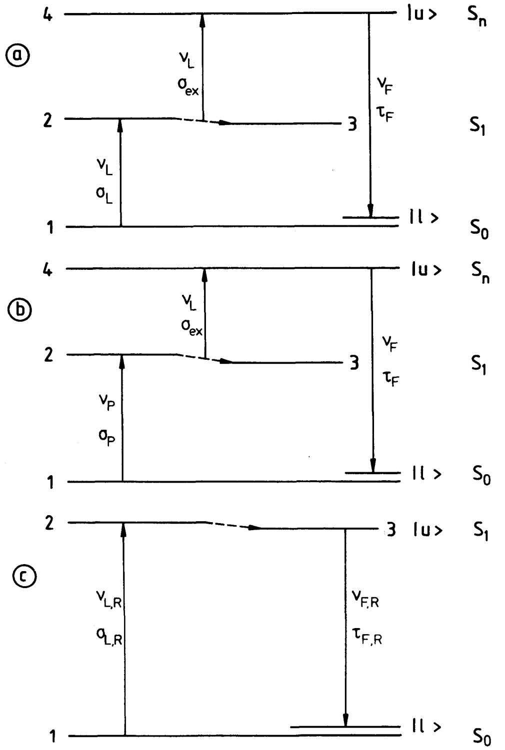

Figure 1 Level schemes for (a) single pulse two-step excitation, (b) double pulse two-step excitation, and (c) single-step excitation of fluorescence emission.

fluorescence emission polarized parallel (field strength $\mathbf{E}_{F\parallel} \parallel \mathbf{E}_L$, intensity $I_{F\parallel}$) or perpendicular ($\mathbf{E}_{F\perp} \perp \mathbf{E}_L$; $I_{F\perp}$) to the pump pulse polarization may be selected with a polarizer or the total emission ($I_F = I_{F\parallel} + I_{F\perp}$) may be measured without a polarizer. The pump pulses promote dye molecules to the upper fluorescence level $|u\rangle$. $\boldsymbol{\mu}_A$ defines the S_1–S_n transition dipole (S_0–S_1 transition dipole for the reference dye) of an excited molecule in level $|u\rangle$. $\boldsymbol{\mu}_E$ denotes the S_n–S_0 (S_1–S_0 in the case of the reference dye) transition dipole moment of the emission. The angle between $\boldsymbol{\mu}_A$ and $\boldsymbol{\mu}_E$ is α. The orientation of $\boldsymbol{\mu}_E$ around $\boldsymbol{\mu}_A$ is isotropic relative to angle β.

2.1. Fluorescence energy

The fluorescence intensity of an emitting dipole $\boldsymbol{\mu}_E$ parallel to the pump pulse polarization is [35–38]

$$dI_{F\parallel} \propto h\nu_F \mu_{Ez}^2 = h\nu_F \mu_E^2 \cos^2 \Theta_E \propto \frac{h\nu_F \cos^2 \Theta_E}{\tau_{rad}} \tag{1}$$

The fluorescence intensity perpendicular to $\mathbf{E}_L$ is

$$dI_{F\perp} \propto h\nu_F \mu_{Ey}^2 = h\nu_F \mu_E^2 \sin^2 \Theta_E \sin^2 \phi_E \propto \frac{h\nu_F (1 - \cos^2 \Theta_E) \sin^2 \phi_E}{\tau_{rad}} \tag{2}$$

Inverse proportionality between μ_E^2 and radiative lifetime τ_{rad} has been applied [39]. The angle Θ_E is related to the angles Θ, α and β of Fig. 2 by the cosine law of spherical trigonometry

$$\cos \Theta_E = \cos \Theta \cos \alpha + \sin \Theta \sin \alpha \cos \beta \tag{3}$$

The fluorescence energy W_F normalized to the input pulse energy W_L is found by integrating dI_F over all molecules in level |u⟩, over the time t', over the solid angle Ω and averaging over the isotropic angular

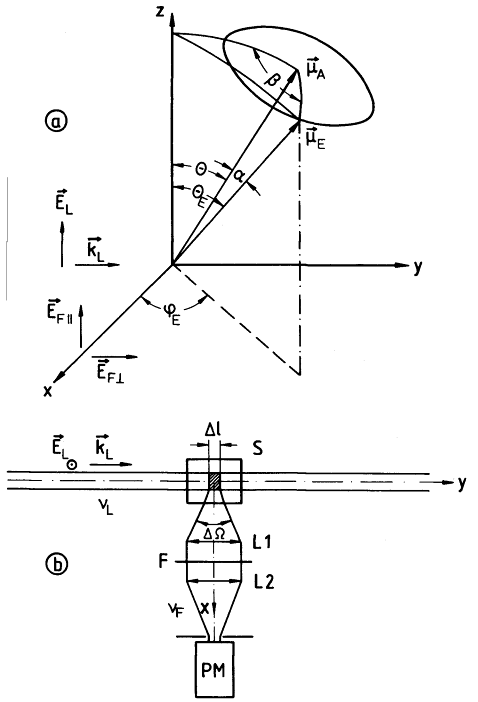

Figure 2 Geometrical arrangement. (a) Orientation of absorption transition dipole moment $\boldsymbol{\mu}_A$ and emission transition dipole moment $\boldsymbol{\mu}_E$ in rectangular coordinate system; (b) fluorescence detection arrangement. S, sample cell; L1, L2, lenses; F, filters.

β distribution. We find

$$\eta_{\parallel}(\alpha) = \frac{W_{F\parallel}(\alpha)}{W_L} = \frac{\Delta\Omega h\bar{\nu}_F}{4\pi W_L n_F^2 \tau_{rad}} \langle \int N_u(\Theta, r, y, t') \cos^2\Theta_E \, d\Omega \, dV \, dt' \rangle_\beta \tag{4a}$$

$$= \frac{\Delta\Omega h\bar{\nu}_F}{4\pi W_L n_F^2 \tau_{rad}} \frac{1}{2\pi} \int_0^{2\pi} d\beta \int_{-\infty}^{\infty} dt' \int_0^{\Delta l} dy \int_0^{\infty} 2\pi r \, dr \int_0^{2\pi} d\phi_E \int_0^{\pi} \sin\Theta$$

$$\times N_u(\Theta, r, y, t') \cos^2\Theta_E \, d\Theta \tag{4b}$$

$$= \frac{\Delta\Omega h\bar{\nu}_F}{4\pi W_L n_F^2 \tau_{rad}} \int_{-\infty}^{\infty} dt' \int_0^{\Delta l} dy \int_0^{\infty} 2\pi r \, dr \, N_u(r, y, t')$$

$$\times \frac{1}{2\pi} \int_0^{2\pi} d\beta \int_0^{2\pi} d\phi_E \int_0^{\pi} s_u(\Theta) \cos^2\Theta_E \sin\Theta \, d\Theta \tag{4c}$$

$$= \frac{\Delta\Omega h\bar{\nu}_F}{4\pi W_L n_F^2 \tau_{rad}} \frac{\int_{-\infty}^{\infty} dt' \int_0^{\Delta l} dy \int_0^{\infty} 2\pi r \, dr \, \bar{N}_u(r, y, t')}{\int_0^{\pi/2} s_u(\Theta) \sin\Theta \, d\Theta}$$

$$\times \frac{1}{2\pi} \int_0^{2\pi} d\beta \int_0^{2\pi} d\phi_E \int_0^{\pi} s_u(\Theta) (\cos^2\Theta \cos^2\alpha + \sin^2\Theta \sin^2\alpha \cos^2\beta) \sin\Theta \, d\Theta \tag{4d}$$

$$= \frac{\Delta\Omega h\bar{\nu}_F}{W_L n_F^2 \tau_{rad}} \frac{M_u}{\int_0^{\pi/2} s_u(\Theta) \sin\Theta \, d\Theta}$$

$$\times \left[\cos^2\alpha \int_0^{\pi/2} s_u(\Theta) \cos^2\Theta \sin\Theta \, d\Theta + \tfrac{1}{2} \sin^2\alpha \int_0^{\pi/2} s_u(\Theta) \sin^3\Theta \, d\Theta \right] \tag{4e}$$

and

$$\eta_\perp(\alpha) = \frac{W_{F\perp}(\alpha)}{W_L} = \frac{\Delta\Omega h\bar{\nu}_F}{4\pi W_L n_F^2 \tau_{rad}} \left\langle \int N_u(\Theta, r, y, t')(1-\cos^2\Theta_E)\sin^2\phi_E \, d\Omega \, dV \, dt' \right\rangle_\beta \tag{5a}$$

$$= \frac{\Delta\Omega h\bar{\nu}_F M_u}{4\pi n_F^2 \tau_{rad} W_L \int_0^{\pi/2} s_u(\Theta)\sin\Theta \, d\Theta} \frac{1}{2\pi} \int_0^{2\pi} d\beta \int_0^{2\pi} d\phi_E \int_0^{\pi} s_u(\Theta)$$

$$\times (1 - \cos^2\Theta\cos^2\alpha - \sin^2\Theta\sin^2\alpha\cos^2\beta)\sin^2\phi_E \sin\Theta \, d\Theta \tag{5b}$$

$$= \frac{\Delta\Omega h\bar{\nu}_F M_u}{n_F^2 \tau_{rad} W_L \int_0^{\pi/2} s_u(\Theta)\sin\Theta \, d\Theta} \left[\frac{1}{2}\int_0^{\pi/2} s_u(\Theta)\sin\Theta \, d\Theta \right.$$

$$\left. - \tfrac{1}{2}\cos^2\alpha \int_0^{\pi/2} s_u(\Theta)\cos^2\Theta\sin\Theta \, d\Theta - \tfrac{1}{4}\sin^2\alpha \int_0^{\pi/2} s_u(\Theta)\sin^3\Theta \, d\Theta \right] \tag{5c}$$

Equation 4 starts from Equation 1 while Equation 5 involves Equation 2. $\Delta\Omega$ is the solid angle accepted by the detection system. $\Delta\Omega/n_F^2$ is the internal acceptance angle in the sample. n_F denotes the mean refractive index of the dye solution in the spectral region of the fluorescence. $\bar{\nu}_F$ is the mean fluorescence frequency. Δl is the length of the fluorescing volume that is imaged to the detector. $N_u(\Theta, r, y, t')$ is the number density of molecules in the upper fluorescence level (dimension cm^{-3}). Going from Equation 4b to 4c and 4d the relation $N_u(\Theta, r, y, t') = N_u(r, y, t')s_u(\Theta) = \bar{N}_u(r, y, t')s_u(\Theta)/\int_0^{\pi/2} s_u(\Theta) \sin\Theta \, d\Theta$ has been used. $s_u(\Theta)$ is the orientational distribution function of the upper fluorescence level population. $\bar{N}_u(r, y, t') = \int_0^{\pi/2} N_u(\Theta, r, y, t') \sin\Theta \, d\Theta = N_u(r, y, t') \int_0^{\pi/2} s_u(\Theta) \sin\Theta \, d\Theta$ is the average number density per steradian. In the step from Equation 4c to 4d $\cos\Theta_E$ is expressed by Equation 3. In Equation 4e the abbreviation

$$M_u = \int_{-\infty}^{\infty} dt' \int_0^{\Delta l} dy \int_0^{\infty} 2\pi r \, dr \, \bar{N}_u(r, y, t') \tag{6}$$

for the space and time integrated population is used. M_u depends on the S_n-state lifetime via the time dependence of $\bar{N}_u$.

The fluorescence energy normalized to the input pulse energy η is related to the fluorescence quantum efficiency q_F by

$$q_F = \frac{\tau_F}{\tau_{rad}} = \frac{n_F^2}{\Delta\Omega} \frac{W_F/\bar{\nu}_F}{W_{abs}/\nu_L} = \frac{n_F^2 \nu_L}{\Delta\Omega \bar{\nu}_F} \frac{\eta}{\kappa} \tag{7}$$

if anisotropy effects are neglected (see Equation 34). $W_{abs} = \kappa W_L$ represents the pulse energy absorbed by S_1–S_n transition (S_0–S_1-transition for reference dye). In the case of double pulse excitation (and in the case of reference excitation) it is $\kappa = 1 - T_E$ where T_E is the energy transmission of the S_1–S_n excitation pulse (and the S_0–S_1 reference excitation pulse).

For a further evaluation of Equations 4e and 5c we have to specify the distribution function $s_u(\Theta)$ of the transition dipole moments $\boldsymbol{\mu}_A$. We distinguish three situations

(i) $s_u(\Theta) = \cos^2\Theta$,
(ii) $s_u(\Theta) = \cos^4\Theta$ and
(iii) $s_u(\Theta) = 1$.

2.1.1. Condition (i) $s_u(\Theta) = \cos^2\Theta$

This condition applies to S_1–S_n absorption starting from an isotropic population in the S_1-state as it is achieved by strongly bleaching the ground state (single and double pulse excitation) or by delaying the

S_1–S_n excitation pulse to allow orientational redistribution (double pulse excitation). The S_n-state has no time for reorientation because of its short lifetime. The condition also applies to S_0–S_1 absorption of reference dyes in highly viscous media ($\tau_{\mathrm{or}} > \tau_{\mathrm{F}}$).

Equations 4e and 5c simplify to

$$\eta_{\parallel}(\alpha) = \frac{\Delta\Omega h\bar{\nu}_{\mathrm{F}}}{n_{\mathrm{F}}^2\tau_{\mathrm{rad}}}\frac{M_{\mathrm{u}}}{W_{\mathrm{L}}}\tfrac{1}{5}[1+2\cos^2\alpha] \tag{8}$$

$$\eta_{\perp}(\alpha) = \frac{\Delta\Omega h\bar{\nu}_{\mathrm{F}}}{n_{\mathrm{F}}^2\tau_{\mathrm{rad}}}\frac{M_{\mathrm{u}}}{W_{\mathrm{L}}}\tfrac{1}{5}[2-\cos^2\alpha] \tag{9}$$

The normalized fluorescence energy detected without polarizers becomes

$$\eta(\alpha) = \eta_{\parallel}(\alpha)+\eta_{\perp}(\alpha) = \frac{\Delta\Omega h\bar{\nu}_{\mathrm{F}}}{n_{\mathrm{F}}^2\tau_{\mathrm{rad}}}\frac{M_{\mathrm{u}}}{W_{\mathrm{L}}}\frac{1}{5}\,[3+\cos^2\alpha] \tag{10}$$

If the absorption and emission transition dipole moments are parallel ($\alpha = 0$) Equation 10 becomes

$$\eta(\alpha=0) = \frac{4}{5}\frac{\Delta\Omega h\bar{\nu}_{\mathrm{F}}}{n_{\mathrm{F}}^2\tau_{\mathrm{rad}}}\frac{M_{\mathrm{u}}}{W_{\mathrm{L}}} \tag{11}$$

In the case of $\alpha = 90^\circ$ Equation 10 reduces to

$$\eta(\alpha=90^\circ) = \frac{3}{5}\frac{\Delta\Omega h\bar{\nu}_{\mathrm{F}}}{n_{\mathrm{F}}^2\tau_{\mathrm{rad}}}\frac{M_{\mathrm{u}}}{W_{\mathrm{L}}} \tag{12}$$

For the reference excitation $\boldsymbol{\mu}_{\mathrm{A}}$ (S_0–S_1 transition dipole) and $\boldsymbol{\mu}_{\mathrm{E}}$ (S_1–S_0 transition dipole) are parallel. For the two-step excitation $\boldsymbol{\mu}_{\mathrm{A}}$($S_1$–$S_n$ transition) and $\boldsymbol{\mu}_{\mathrm{E}}$($S_n$–$S_0$ transition) may have any angle between $0 \leqslant \alpha \leqslant 90^\circ$ (preferably 0 and 90°). The detected fluorescence signal depends only slightly on the angle between the absorption and emission dipole moment [$\eta(\alpha = 90^\circ)/\eta(\alpha = 0) = 3/4$]. This fact allows the S_n-state lifetime measurement τ_{F} to be determined without a knowledge of the angle α.

2.1.2. Condition (ii) $s_{\mathrm{u}}(\theta) = \cos^4\Theta$

This condition is approximately fulfilled for S_1–S_n absorption starting from the weakly populated S_1-state (S_1-state distributions $\propto \cos^2\Theta$) prior to reorientation of the S_1-state and $\boldsymbol{\mu}(S_0\text{–}S_1) \parallel \boldsymbol{\mu}(S_1\text{–}S_n)$. The situation $\boldsymbol{\mu}(S_0\text{–}S_n) \parallel \boldsymbol{\mu}_{\mathrm{A}}$ and $\sphericalangle(\boldsymbol{\mu}_{\mathrm{A}}, \boldsymbol{\mu}_{\mathrm{E}}) = \alpha$ is equivalent to $\sphericalangle[\boldsymbol{\mu}(S_0\text{–}S_1), \boldsymbol{\mu}_{\mathrm{A}}] = \alpha$ and $\boldsymbol{\mu}_{\mathrm{A}} \parallel \boldsymbol{\mu}_{\mathrm{E}}$.

Equations 4e and 5c reduce to

$$\eta_{\parallel}(\alpha) = \frac{\Delta\Omega h\bar{\nu}_{\mathrm{F}}}{n_{\mathrm{F}}^2\tau_{\mathrm{rad}}}\frac{M_{\mathrm{u}}}{W_{\mathrm{L}}}\frac{1}{7}\,[1+4\cos^2\alpha] \tag{13}$$

$$\eta_{\perp}(\alpha) = \frac{\Delta\Omega h\bar{\nu}_{\mathrm{F}}}{n_{\mathrm{F}}^2\tau_{\mathrm{rad}}}\frac{M_{\mathrm{u}}}{W_{\mathrm{L}}}\frac{1}{7}\,[3-2\cos^2\alpha] \tag{14}$$

The unpolarized fluorescence energy becomes

$$\eta(\alpha) = \frac{\Delta\Omega h\bar{\nu}_{\mathrm{F}}}{n_{\mathrm{F}}^2\tau_{\mathrm{rad}}}\frac{M_{\mathrm{u}}}{W_{\mathrm{L}}}\frac{2}{7}\,[2+\cos^2\alpha] \tag{15}$$

For $\alpha = 0$ we find

$$\eta(\alpha = 0^\circ) = \frac{6}{7}\frac{\Delta\Omega h\bar{\nu}_{\mathrm{F}}}{n_{\mathrm{F}}^2\tau_{\mathrm{rad}}}\frac{M_{\mathrm{u}}}{W_{\mathrm{L}}} \tag{16}$$

while for $\alpha = 90^\circ$ the result is

$$\eta(\alpha = 90^\circ) = \frac{4}{7}\frac{\Delta\Omega h\bar{\nu}_{\mathrm{F}}}{n_{\mathrm{F}}^2\tau_{\mathrm{rad}}}\frac{M_{\mathrm{u}}}{W_{\mathrm{L}}} \tag{17}$$

Again the ratio $\eta(\alpha = 90^\circ)/\eta(\alpha = 0) = 2/3$ is near to 1.

2.1.3. Condition (iii) $s_u(\Theta) = 1$

This condition applies to the reference dyes with $\tau_{or} \ll \tau_F$ as is the case in low viscous solvents. Equations 4e and 5c become

$$\eta_{\parallel}(\alpha) = \eta_{\perp}(\alpha) = \frac{1}{3}\,\frac{\Delta\Omega h\bar{\nu}_F}{n_F^2 \tau_{rad}}\,\frac{M_u}{W_L} \tag{18}$$

The fluorescence emission is independent of the polarization and angle α.

The total normalized fluorescence energy is

$$\eta(\alpha) = \eta_{\parallel}(\alpha) + \eta_{\perp}(\alpha) = \frac{2}{3}\,\frac{\Delta\Omega h\bar{\nu}_F}{n_F^2 \tau_{rad}}\,\frac{M_u}{W_L} \tag{19}$$

Comparing cases (i) to (iii) we find only a weak dependence on the orientational distribution of the upper fluorescence level, i.e.

$$\eta(\alpha = 0, \cos^2\Theta) : \eta(\alpha = 0, \cos^4\Theta) : \eta(\alpha = 0, 1) = \tfrac{4}{5} : \tfrac{6}{7} : \tfrac{2}{3}$$

and

$$\eta(\alpha = 90^\circ, \cos^2\Theta) : \eta(\alpha = 90^\circ, \cos^4\Theta) : \eta(\alpha = 90^\circ, 1) = \tfrac{3}{5} : \tfrac{4}{7} : \tfrac{2}{3}$$

The fact that the fluorescence signal detected without polarizer is nearly independent of the orientation of the specific absorption and emission dipole moments allows easy S_n-state lifetime determination from fluorescence signal measurements without a knowledge of the orientation of the transition dipoles.

For the discussed cases of population anisotropy and angle between absorption and emission the total normalized fluorescence energy may be written as

$$\eta(\alpha) = \frac{\Delta\Omega h\bar{\nu}_F}{n_F^2 \tau_{rad}}\,\frac{M_u}{W_L}\,A(s_u, \alpha) \tag{20}$$

with $0.571 \leqslant A(s_u, \alpha) \leqslant 0.857$.

The radiative lifetime τ_{rad} for the S_n–S_0 transitions is found by measuring the S_n–S_0 fluorescence spectral distribution $E(\lambda)$ (quantum distribution $\int E(\lambda)\mathrm{d}\lambda = 1$) and the S_0–S_n absorption cross-section $\sigma(\lambda)$ according to the Strickler–Berg formula [25, 40]

$$\tau_{rad}^{-1} = \frac{8\pi c n_F^3}{n_A}\,\frac{\int E(\lambda)\mathrm{d}\lambda}{\int E(\lambda)\lambda^4 \mathrm{d}\lambda}\int \frac{\sigma(\lambda)}{\lambda}\mathrm{d}\lambda \tag{21}$$

c is the vacuum light velocity. The radiative lifetime for the S_1–S_0 transition of the reference may be determined from the Strickler–Berg formula or obtained from direct measurement of the fluorescence lifetime $\tau_{F,R}$ ($\tau_{rad,R} = \tau_{F,R}/q_{F,R}$, Equation 7).

2.2. Time integrated upper fluorescence level population

The ratio M_u/W_L depends on the S_n-state lifetime τ_F. An explicit expression of M_u/W_L that reveals the τ_F dependence has to be found. Here three cases are distinguished:

(i) the single pulse two-step S_n excitation
(ii) the double pulse S_n excitation and
(iii) the single-step S_1 reference excitation.

In the single-pulse two-step excitation technique the population density N_u has to be determined by nonlinear transmission measurements including the determination of the S_1–S_n excited state absorption cross-section. In the double pulse excitation technique, the absorption of the S_1–S_n excitation pulse has to be determined. In the single-step fluorescence excitation of the reference the absorption of the S_1 excitation pulse has to be measured.

2.2.1. Single pulse two-step S_0–S_1–S_n excitation

To obtain the level population density N_u of the S_n state the nonlinear transmission of the pump pulse through the dye sample has to be measured and compared with calculations of the energy transmission through the dye [9, 27, 41].

For the level system of Fig. 1a the light propagation through the dye is described by the following equation system

$$\frac{\partial N_1(\Theta)}{\mathrm{d}t'} = -\frac{3\sigma_L I_L}{h\nu_L}\,[N_1(\Theta)-N_2(\Theta)]\,\cos^2\Theta + \frac{1}{\tau_{S1}}\,[N_2(\Theta)+N_3(\Theta)] + k_{41}N_4(\Theta) - \frac{1}{\tau_{or}}\,[N_1(\Theta)-\bar{N}_1] \tag{22}$$

$$\frac{\partial N_2(\Theta)}{\partial t'} = \frac{I_L}{h\nu_L}\left\{3\sigma_L[N_1(\Theta)-N_2(\Theta)]\,\cos^2\Theta - \sigma_{ex}\left[N_2(\Theta)-N_4(\Theta)\frac{N_2(\Theta)}{N_2(\Theta)+N_3(\Theta)}\right]\right\} - \left(\frac{1}{\tau_{FC}}+\frac{1}{\tau_{S1}}\right)N_2(\Theta) - \frac{1}{\tau_{or}}\,[N_2(\Theta)-\bar{N}_2] \tag{23}$$

$$\frac{\partial N_3(\Theta)}{\partial t'} = -\frac{\sigma_{ex} I_L}{h\nu_L}\left[N_3(\Theta)-N_4(\Theta)\frac{N_3(\Theta)}{N_3(\Theta)+N_4(\Theta)}\right] + \frac{1}{\tau_{FC}}N_2(\Theta) - \frac{1}{\tau_{S1}}N_3(\Theta) + k_{43}N_4(\Theta) - \frac{1}{\tau_{or}}\,[N_3(\Theta)-\bar{N}_3] \tag{24}$$

$$\frac{\partial N_4(\Theta)}{\partial t'} = \frac{\sigma_{ex} I_L}{h\nu_L}\,[N_2(\Theta)+N_3(\Theta)-N_4(\Theta)] - k_4 N_4(\Theta) - \frac{1}{\tau_{or}}\,[N_4(\Theta)-\bar{N}_4] \tag{25}$$

$$\bar{N}_i = \int_0^{\pi/2} N_i(\Theta)\sin\Theta\,\mathrm{d}\Theta \qquad (i = 1 \text{ to } 4) \tag{26}$$

$$\frac{\partial I_L}{\partial z} = -I_L\left\{3\sigma_L\int_0^{\pi/2}[N_1(\Theta)-N_2(\Theta)]\,\cos^2\Theta\sin\Theta\,\mathrm{d}\Theta + \sigma_{ex}(\bar{N}_2+\bar{N}_3)\right\} \tag{27}$$

The coordinate transformation $t' = t - nz/c$ is used (n, refractive index). The population number densities (dimension cm^{-3}) are $N_1(\Theta), N_2(\Theta), N_3(\Theta)$, and $N_4(\Theta) = N_u(\Theta)$. The initial conditions for the number densities are $N_1(\Theta, t' = -\infty, y, r) = N_0 = -\ln(T_0)/(\sigma_L l)$, $N_2(\Theta, t' = -\infty, y, r) = N_3(\Theta, t' = -\infty, y, r) = N_4(\Theta, t' = -\infty, y, r) = 0$. N_0 is the number density of dissolved dye molecules. T_0 is the small signal dye transmission and l the sample length. The initial condition for the laser intensity is $I_L(t', r, y = 0) = I_{0L}\exp(-t'^2/t_0^2)\exp(-r^2/r_0^2)$. The $1/e$ width t_0 of the pulse duration is related to the FWHM value Δt_L by $t_0 = \Delta t_L/[2(\ln 2)^{1/2}]$. The angular anisotropy of ground state absorption is taken into account by $\sigma_L(\Theta) = 3\sigma_L\cos^2\Theta$ [9, 27]. For the excited state absorption only the orientationally averaged cross-section σ_{ex} is used in the equation system. The last term in Equation 27 includes excited state absorption from level 4 (= $|u\rangle$) to higher lying states (open system). τ_{S1} is the lifetime of level 3. τ_{FC} represents the relaxation time from the excited Franck–Condon level 2 to the relaxed level 3. The relaxation rates k_{43} and k_{41} ($k_4 = \tau_F^{-1} = k_{43} + k_{41}$) describe the relaxation of level 4 to level 3 and 1, respectively. τ_{or} is the molecular reorientation time.

Equation system 22–27 is solved numerically. The experimentally measured energy transmission $T_E = W_L(l)/W_L$ is related to the input and output intensity distribution by

$$T_E = \frac{\int_0^\infty\int_{-\infty}^\infty I_L(r, t', l)\,\mathrm{d}t'\,2\pi r\,\mathrm{d}r}{I_{0L}\int_0^\infty 2\pi r\exp(-r^2/r_0^2)\,\mathrm{d}r\int_{-\infty}^\infty\exp(-t'^2/t_0^2)\,\mathrm{d}t'} = \frac{2\pi\int_0^\infty\int_{-\infty}^\infty I_L(r, t', l)\,\mathrm{d}t' r\,\mathrm{d}r}{\pi^{3/2} r_0^2 t_0 I_{0L}} \tag{28}$$

The energy transmission at high input intensities is limited by the excited state absorption. σ_{ex} is determined by fitting the calculations to the experimental data. σ_{ex} depends slightly on the S_n-state lifetime τ_F. The S_n-level population density $N_u = N_4$ is obtained from Equation 25 as a function of τ_F. The time and space integrated population M_u is calculated using Equation 6.

2.2.2. Double pulse two-step excitation

Referring to Fig. 1b, the total population of the upper fluorescence level is determined by the number of photons absorbed in the S_1–S_n transition process. It is

$$\int_0^{\Delta l} \mathrm{d}y \int_0^{\infty} 2\pi r \, \mathrm{d}r \, \bar{N}_u(r, y, t') = \frac{1}{h\nu_L} \int_{\tilde{t}'=-\infty}^{t'} \mathrm{d}W_{\mathrm{abs}}(\tilde{t}') \exp\left(-(t' - \tilde{t}')/\tau_F\right) \tag{29}$$

$W_{\mathrm{abs}}(t') = \int_{\tilde{t}'=-\infty}^{t'} \mathrm{d}W_{\mathrm{abs}}(\tilde{t}')$ is the absorbed pulse energy of frequency ν_L up to time t'. Insertion of Equation 29 into Equation 6 gives

$$M_u = \int_{t'=-\infty}^{\infty} \mathrm{d}t' \frac{1}{h\nu_L} \int_{\tilde{t}'=-\infty}^{t'} \mathrm{d}W_{\mathrm{abs}}(\tilde{t}') \exp\left[-(t' - \tilde{t}')/\tau_F\right] \tag{30}$$

Changing the succession of integration leads to

$$M_u = \frac{1}{h\nu_L} \int_{\tilde{t}'=-\infty}^{\infty} \mathrm{d}W_{\mathrm{abs}}(\tilde{t}') \int_{t'=\tilde{t}'}^{\infty} \exp\left[-(t' - \tilde{t}')/\tau_F\right] \mathrm{d}t' \tag{31a}$$

$$= \frac{\tau_F}{h\nu_L} \int_{\tilde{t}'=-\infty}^{\infty} \mathrm{d}W_{\mathrm{abs}}(\tilde{t}') \tag{31b}$$

$$= \frac{\tau_F}{h\nu_L} W_{\mathrm{abs}} \tag{31c}$$

$$= \frac{\tau_F}{h\nu_L} W_L(1 - T_E) \tag{31d}$$

The quantity M_u/W_L becomes

$$\frac{M_u}{W_L} = \frac{\tau_F(1 - T_E)}{h\nu_L} \tag{32}$$

which is directly proportional to the S_n-state lifetime τ_F. The energy transmission T_E of the S_1–S_n excitation pulse is easily measured by transmission detection.

2.2.3. Single-step S_0–S_1 excitation

The mathematical description of S_0–S_1 absorption of the reference dye is identical to the S_1–S_n absorption description of Section 2.2.2 and Equation 32 applies. Using the parameters of Fig. 1c Equation 32 reads

$$\frac{M_{u,R}}{W_{L,R}} = \frac{\tau_{F,R}(1 - T_{E,R})}{h\nu_{L,R}} \tag{33}$$

Insertion of Equation 33 into Equation 20 gives

$$\eta_R(0) = \frac{\Delta\Omega \bar{\nu}_{F,R} q_{F,R}(1 - T_{E,R})}{n_{F,R}^2 \nu_{L,R}} A_R(s_u, 0) \tag{34}$$

where $q_{F,R} = \tau_{F,R}/\tau_{\mathrm{rad},R}$ is the S_1–S_0 fluorescence quantum yield (see Equation 7). The angle between the S_0–S_1 absorption and the S_1–S_0 emission dipole moment is $\alpha = 0$.

2.3. S_n–S_0 fluorescence normalized to S_1–S_0 reference fluorescence

The ratio of S_n–S_0 fluorescence of the investigated dye to S_1–S_0 fluorescence of the reference dye, in the case of single pulse two-step excitation, is

$$\frac{\eta(\alpha)}{\eta_R(0)} = \frac{h\bar{\nu}_F \nu_{L,R} n_{F,R}^2}{\bar{\nu}_{F,R} n_F^2 q_{F,R}(1-T_{E,R})\tau_{\mathrm{rad}}} \frac{M_u}{W_L} \frac{A(s_u,\alpha)}{A_R(s_u,0)} \tag{35}$$

while in the case of double pulse excitation we find

$$\frac{\eta(\alpha)}{\eta_R(0)} = \frac{\bar{\nu}_F \tau_F(1-T_E)\nu_{L,R} n_{F,R}^2}{\nu_L n_F^2 \tau_{\mathrm{rad}} \bar{\nu}_{F,R} q_{F,R}(1-T_{E,R})} \frac{A(s_u,\alpha)}{A_R(s_u,0)} \tag{36a}$$

$$= \frac{\bar{\nu}_F \nu_{L,R} n_{F,R}^2 (1-T_E) A(s_u,\alpha)}{\bar{\nu}_{F,R}\nu_L n_F^2(1-T_{E,R}) A_R(s_u,0)} \frac{q_F}{q_{F,R}} \tag{36b}$$

Equations 35 and 36a are used to determine τ_F in the experiments.

2.4. Disturbance of impurity fluorescence excited by two-photon absorption

In the direct single pulse one-photon excitation of the S_n-state, the S_n–S_0 fluorescence quantum yield measurement is disturbed by one-photon excited S_1–S_0 fluorescence of impurity molecules. The smaller the S_n–S_0 quantum yield, the more disturbing is the S_1–S_0 impurity fluorescence. In the two-step excitation processes of S_n–S_0 fluorescence the S_1-state of the disturbing impurity molecules can only be populated by two-photon absorption without an intermediate state.

Referring to the level system of Fig. 1c and neglecting a depopulation of the ground state by two-photon absorption the population number density N_{uI} of the fluorescing S_1-impurity level is determined by

$$\frac{\partial N_{uI}}{\partial t'} = \frac{\sigma_I^{(2)} N_I I_L^2}{(h\nu_L)^2} - \frac{N_{uI}}{\tau_I} \tag{37}$$

N_I is the total number density of impurity molecules which are involved in the S_0–S_1 two-photon absorption at laser frequency ν_L. $\sigma_I^{(2)}$ is the two-photon absorption cross-section of the impurity molecules at ν_L. τ_I is the S_1-state lifetime of the impurity molecules. The solution of Equation 37 is

$$N_{uI}(t') = \frac{\sigma_I^{(2)} N_I}{(h\nu_L)^2} \int_{-\infty}^{t'} I_L^2(\tilde{t}') \exp\left[-(t'-\tilde{t}')/\tau_I\right] \mathrm{d}\tilde{t}' \tag{38}$$

The total time-integrated population of the upper impurity fluorescence level M_{uI} is

$$M_{uI} = \int_{-\infty}^{\infty} \mathrm{d}t' \int_0^{\Delta l} \mathrm{d}y \int_0^{\infty} 2\pi r\, \mathrm{d}r\, N_{uI}(r,y,t') \tag{39a}$$

$$= \frac{\sigma_I^{(2)} N_I}{(h\nu_L)^2} \int_0^{\Delta l} \mathrm{d}y \int_0^{\infty} 2\pi r\, \mathrm{d}r \int_{\tilde{t}'=-\infty}^{\infty} \mathrm{d}\tilde{t}' I_L^2(\tilde{t}') \int_{t'=\tilde{t}'}^{\infty} \exp\left[-(t'-\tilde{t}')/\tau_I\right] \mathrm{d}t' \tag{39b}$$

$$= \frac{\tau_I \sigma_I^{(2)} N_I}{(h\nu_L)^2} \int_0^{\Delta l} \mathrm{d}y \int_0^{\infty} 2\pi r\, \mathrm{d}r \int_{-\infty}^{\infty} I_L^2(y,r,t')\, \mathrm{d}t' \tag{39c}$$

Proceeding from Equation 39a to 39b the sequence of integration is changed.

Approximating the integral $\int_0^{\Delta l} I_L^2(y,r,t')\mathrm{d}y$ by $[I_L(0,r,t')(1+T_E)/2]^2 \Delta l$ and setting $I_L(0,r,t') = I_{OL}\exp(-r^2/r_0^2)\exp(-t^2/t_0^2)$ Equation 39c reduces to

$$M_{uI} = \frac{\tau_I \sigma_I^{(2)} N_I}{(h\nu_L)^2} \frac{(1+T_E)^2}{4} \frac{I_{OL}\Delta l}{2^{3/2}} W_L \tag{40}$$

and the normalized fluorescence energy $\eta_{\mathrm{I}} = W_{\mathrm{F,I}}/W_{\mathrm{L}}$ becomes by insertion of Equation 40 into Equation 20 (without the anisotropy factor):

$$\eta_{\mathrm{I}} = \frac{\Delta\Omega\bar{\nu}_{\mathrm{F,I}}q_{\mathrm{F,I}}\sigma_{\mathrm{I}}^{(2)}N_{\mathrm{I}}(1+T_{\mathrm{E}})^2 I_{\mathrm{OL}}\Delta l}{2^{7/2}n_{\mathrm{F}}^2 h\nu_{\mathrm{L}}^2} \tag{41}$$

$q_{\mathrm{F,I}} = \tau_{\mathrm{I}}/\tau_{\mathrm{rad,I}}$ is the S_1–S_0 fluorescence quantum yield of the impurity molecules.

The ratio of two-photon excited S_1–S_0 impurity fluorescence to two-step excited S_n–S_0 fluorescence of the dye under investigation is, in the case of single pulse excitation

$$\frac{\eta_{\mathrm{I}}}{\eta(\alpha)} = \frac{q_{\mathrm{F,I}}\sigma_{\mathrm{I}}^{(2)}N_{\mathrm{I}}I_{\mathrm{OL}}\bar{\nu}_{\mathrm{F,I}}(1+T_{\mathrm{E}})^2\Delta l\,\tau_{\mathrm{rad}}}{2^{7/2}h^2\bar{\nu}_{\mathrm{F}}\nu_{\mathrm{L}}^2(M_{\mathrm{u}}/W_{\mathrm{L}})A(s_{\mathrm{u}},\alpha)} \tag{42}$$

In the case of double pulse excitation with two-photon induced impurity fluorescence by the pump pulse of frequency ν_{p} the ratio is (Fig. 1b, Equations 41, 20 and 32)

$$\frac{\eta_{\mathrm{I}}}{\eta(\alpha)} = \frac{q_{\mathrm{F,I}}\sigma_{\mathrm{I}}^{(2)}N_{\mathrm{I}}I_{\mathrm{OP}}\bar{\nu}_{\mathrm{F,I}}\nu_{\mathrm{L}}(1+T_{\mathrm{E}})^2\Delta l}{2^{7/2}h\bar{\nu}_{\mathrm{F}}\nu_{\mathrm{P}}^2(1-T_{\mathrm{E}})q_{\mathrm{F}}A(s_{\mathrm{u}},\alpha)} \tag{43}$$

Equations 42 and 43 allow judgement of the influence of impurity fluorescence in the S_n–S_0 fluorescence measurements. The contribution of impurity fluorescence relative to S_n–S_0 fluorescence grows with

(i) the fluorescence quantum efficiency of the impurity molecules $q_{\mathrm{F,I}}$
(ii) the two-photon absorption cross-section $\sigma_{\mathrm{I}}^{(2)}$
(iii) the concentration of impurity molecules N_{I}
(iv) the pump pulse intensity I_{OL} or I_{OP} and
(v) the inverse quantum efficiency of S_n–S_0 dye fluorescence $q_{\mathrm{F}}^{-1} = \tau_{\mathrm{rad}}/\tau_{\mathrm{F}}$.

In the experiments it may be checked whether impurity fluorescence plays a decisive role by measuring the intensity dependence of the observed fluorescence signal. The two-photon excited impurity fluorescence and the two-step excited S_n–S_0 fluorescence are proportional to I_{OL}^2 at low intensities, but at high intensities the two-step excited S_n–S_0 fluorescence saturates while the impurity fluorescence remains proportional I_{OL}^2 (two-step absorption cross-section greater than two-photon absorption cross-section). Saturation of two-photon absorption may be estimated by calculating $N_{\mathrm{uI}}(t')/N_{\mathrm{I}}$ with the aid of Equation 38.

3. Experiments

In the experiments we investigated Kodak mode-locking dyes 9740 and 9860 for Nd-lasers. The fast mode-locking dye 5 from Kodak and Lambda Physik was investigated in [41] and some results are included here. The absorption spectra of dyes 9740 and 9860 are shown in Figs. 3 and 4 respectively.

The single pulse two-step excitation process was used to populate the S_4 level of the dyes around 530 nm. This technique requires energy transmission measurements (determination of upper fluorescence level population) and S_4–S_0 fluorescence yield measurements.

The experimental arrangement is shown in Fig. 5. Single picosecond light pulses from a mode-locked Nd-phosphate glass laser were applied. The laser pulses (wavelength 1.053 μm, duration $\Delta t_{\mathrm{L}} \simeq 5$ ps FWHM) were slightly focused with lens L1 to the sample cell S. Dye samples with initial transmission $T_0 = 0.01$ were applied. The energy transmission was detected with vacuum photocells PD1 and PD3. The input peak intensity was obtained by energy transmission measurement through the saturable absorber 9860 of initial transmission $T_0 = 0.173$ [42]. The peak intensity calibration curve is shown dotted in Fig. 6.

The measured energy transmission data are depicted in Figs. 6 and 7 for dyes 9860 and 9740 respectively. They were used to determine the S_1–S_4 excited-state absorption cross-sections σ_{ex}. The curves

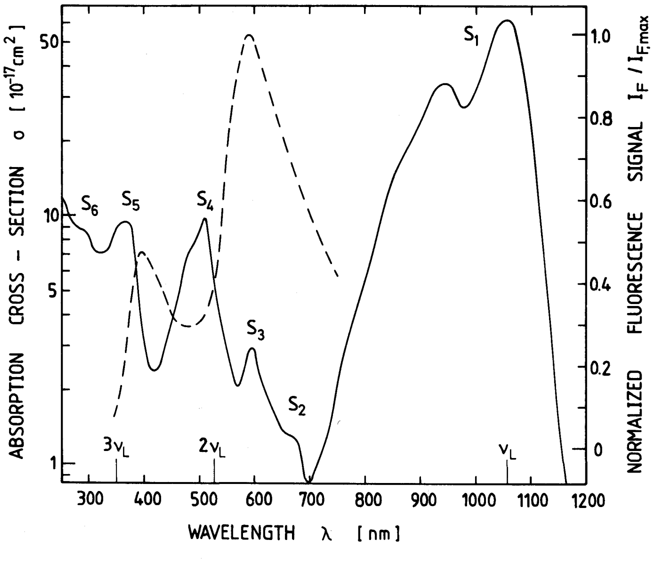

Figure 3 Absorption spectrum of dye 9740 together with normalized S_n–S_0 fluorescence spectrum.

were calculated using Equation system 22–28 and the dye parameters listed in Table I (laser parameters: $\nu_L = 9497\ \mathrm{cm}^{-1}$, $\Delta t_L = 5$ ps, temporal and spatial gaussian shape). The S_0–S_1 ground-state absorption cross-sections σ_L were obtained from spectrophotometer measurements (Figs. 3 and 4). The S_1–S_0 absorption recovery times τ_{S1} were taken from the literature [43, 44]. The Franck–Condon relaxation time τ_{FC} from level 2 to 3 was assumed to be $\tau_{FC} = 0.7$ ps [45, 46]. The relaxation of the excited level 4 was assumed to proceed via level 3, i.e. the rates were $\tau_F^{-1} = k_4 = k_{41} + k_{43}, k_{41} = 0$. The solid curves were calculated for a fixed relaxation rate $\tau_F = 10^{-13}$ s and varying excited state absorption cross-section σ_{ex}. For the dashed curves τ_F was varied and σ_{ex} was fixed.

The S_4-state lifetime τ_F of the dyes investigated was deduced from S_4–S_0 fluorescence signal measurements. The ratio of the normalized S_4–S_0 fluorescence to the normalized S_1–S_0 fluorescence of the reference was measured. Rhodamine 6G dissolved in ethanol was used as reference. The rhodamine 6G parameters are listed in Table II.

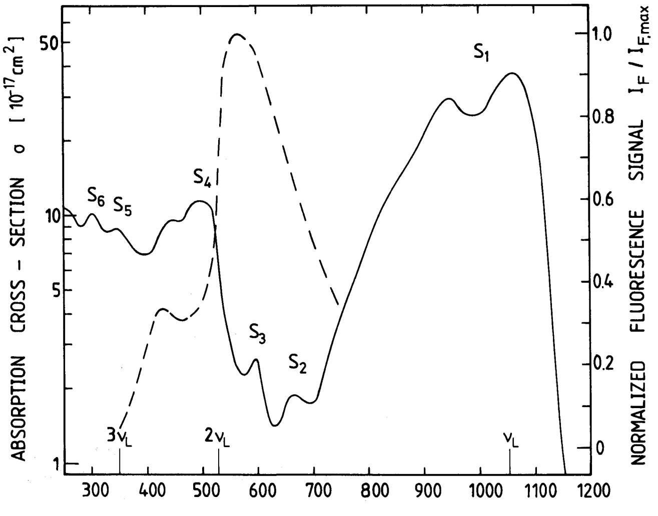

Figure 4 Absorption and normalized emission spectra of dye 9860.

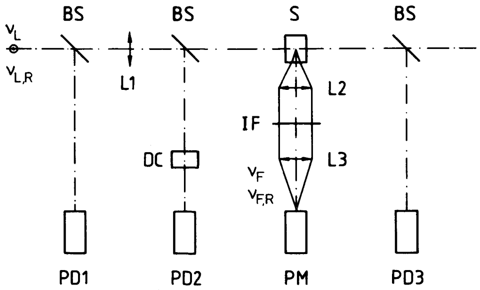

Figure 5 Experimental arrangement. BS, beam splitters; L1–L3, lenses (f_1 = 70 cm, f_2 = 5 cm, f_3 = 10 cm); S, sample; IF, interference filter; DC, saturable absorber cell for intensity detection; PD1–PD3, photodetectors; PM, photomultiplier.

The fluorescence detection arrangement is shown in Fig. 5. The fluorescence signal was observed under 90° to the pump pulse propagation with photomultiplier PM. No polarizer was inserted in the fluorescence path. An interference filter selected the fluorescence spectral region. The pump light was polarized perpendicular to the observation direction. For the measurement of the reference fluorescence signal second harmonic light pulses were generated in a KDP crystal. The fundamental frequency was filtered out and the polarization of the second harmonic was rotated to the vertical direction with a half-wave plate. The second harmonic pulses were attenuated in order not to bleach the reference dye, i.e. $T_{E,R} = T_{0,R}$ and η_R was independent of reference pump pulse intensity.

The measured η/η_R values were used to calculate the corresponding M_u/W_L values with the aid of Equation 35 where $A(s_u, \alpha)/A_R(s_u, 0) = 1$ was assumed. Figs. 8 and 9 depict the M_u/W_L values obtained for dyes 9740 and 9860 respectively. The M_u/W_L curves were calculated using Equation 6 whereby $\bar{N}_u(r, y, t') = \bar{N}_4(r, y, t')$ was obtained from Equation system 22–27. The best-fit S$_4$-state lifetimes τ_F were around 60 fs. They are listed in Table I.

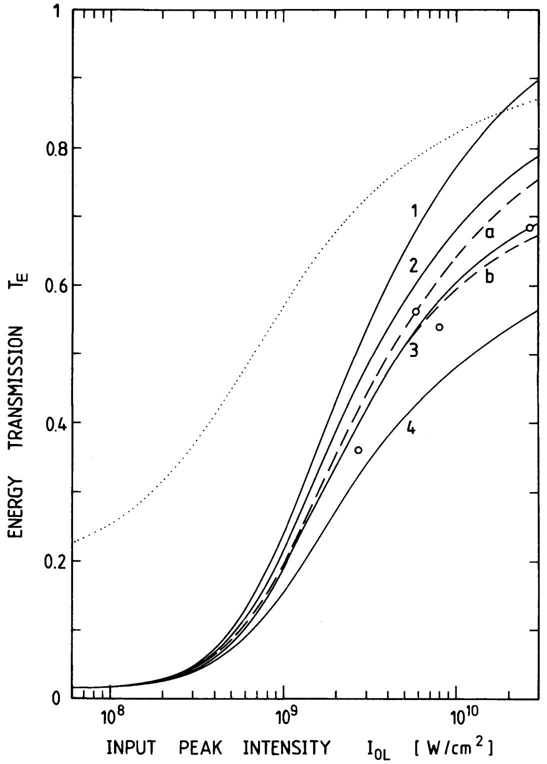

Figure 6 Energy transmission through dye 9860. Pulse duration Δt_L = 5 ps. Dye parameters listed in Table I. Solid curves: $\tau_F = k_{43}^{-1} = 10^{-13}$ s, and 1, $\sigma_{ex} = 0$; 2, $\sigma_{ex} = 1.25 \times 10^{-17}$ cm^2; 3, $\sigma_{ex} = 2.5 \times 10^{-17}$ cm^2; 4, $\sigma_{ex} = 5 \times 10^{-17}$ cm^2. Dashed curves: $\sigma_{ex} = 2.5 \times 10^{-17}$ cm^2, and a, $\tau_F = 10^{-12}$ s; b, $\tau_F = 10^{-14}$ s. Dotted curve: calibration curve for intensity detection (T_0 = 0.173, $\tau_F = 10^{-13}$ s, $\sigma_{ex} = 2.5 \times 10^{-17}$ cm^2).

TABLE I Parameters of the dyes investigated; solvent 1,2-dichloroethane; room temperature; pump laser frequency $\nu_L = 9497\ \text{cm}^{-1}$; two-step excitation $S_0 \rightarrow S_1 \rightarrow S_4$

Parameter	No. 5	No. 9470	No. 9860
σ_L [cm^2]	3×10^{-16}	6.1×10^{-16}	3.7×10^{-16}
σ_{ex} [cm^2]	6×10^{-17}	3.5×10^{-17}	2.5×10^{-17}
τ_{S_1} [ps]	2.7*	11†	7*†
τ_F [fs]	60 ± 20	65 ± 25	55 ± 20
τ_{FC} [ps]	0.7	0.7	0.7
τ_{or} [ps]	150	150	150
τ_{rad} [ns]	9.2	9.6	4.9
$\bar{\nu}_F$ [cm^{-1}]	17 500	16 700	17 100
P	0.17	0.03	0.06
$n_A \simeq n_F$	1.45	1.45	1.45
T_0	0.01	0.01	0.01

* [43]
† [44]

TABLE II Parameters of reference dye rhodamine 6G dissolved in ethanol; room temperature; pump laser frequency $\nu_{L,R} = 18\,994\ \text{cm}^{-1}$; single-step excitation $S_0 \rightarrow S_1$

Parameter	Value
$\tau_{F,R}$	4.2 ns*†
$q_{F,R}$	0.88*
τ_{or}	270 ps‡
$\bar{\nu}_F$	17 600 cm^{-1}
$n_{F,R}$	1.37
P	0
T_0	0.9

* [47]
† [8]
‡ [48]

The S_4–S_0 radiative lifetimes needed in Equation 35 we obtained from the S_0–S_4 absorption and S_4–S_0 emission spectra and application of the Strickler–Berg formula (Equation 21). The normalized S_n–S_0 emission spectra of the dyes are included in Figs. 3 and 4. They were measured with a spectrometer in front of the photomultiplier and without a polarizer in the fluorescence path. The S_5–S_0 fluorescence observed is due to the S_5 level population by S_4–S_5 excited state absorption.

The polarization degree $P = (W_{F\parallel} - W_{F\perp})/(W_{F\parallel} + W_{F\perp})$ was detected with a dichroic sheet in the fluorescence path. The values obtained are reported in Tables I and II. The S_4–S_0 polarization degree

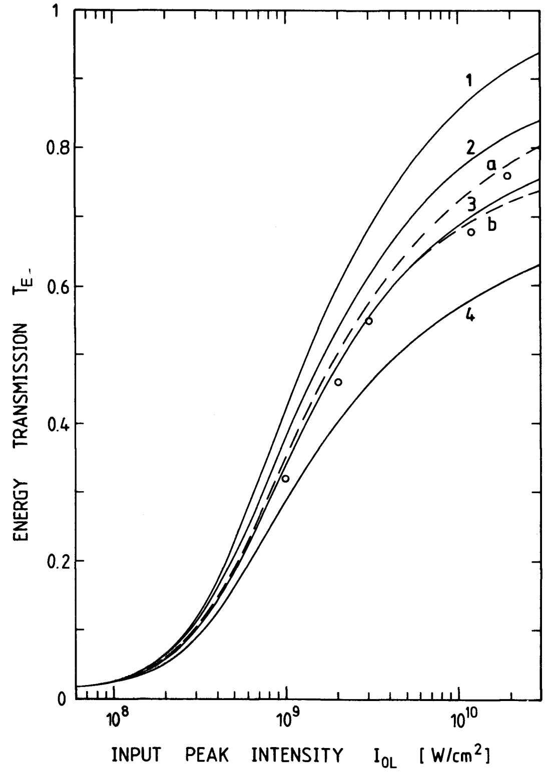

Figure 7 Energy transmission through dye 9740. Laser parameters $\Delta t_L = 5$ ps, frequency $\nu_L = 9497\ \text{cm}^{-1}$. Dye parameters listed in Table I. Solid curves: $\tau_F = k_4^{-1} = k_{43}^{-1} = 10^{-13}$ s, and 1, $\sigma_{ex} = 0$; 2, $\sigma_{ex} = 1.75 \times 10^{-17}\ \text{cm}^2$; 3, $\sigma_{ex} = 3.5 \times 10^{-17}\ \text{cm}^2$; 4, $\sigma_{ex} = 7 \times 10^{-17}\ \text{cm}^2$. Dashed curves: $\sigma_{ex} = 3.5 \times 10^{-17}\ \text{cm}^2$, and a, $\tau_F = 10^{-12}$ s; b, $\tau_F = 10^{-14}$ s.

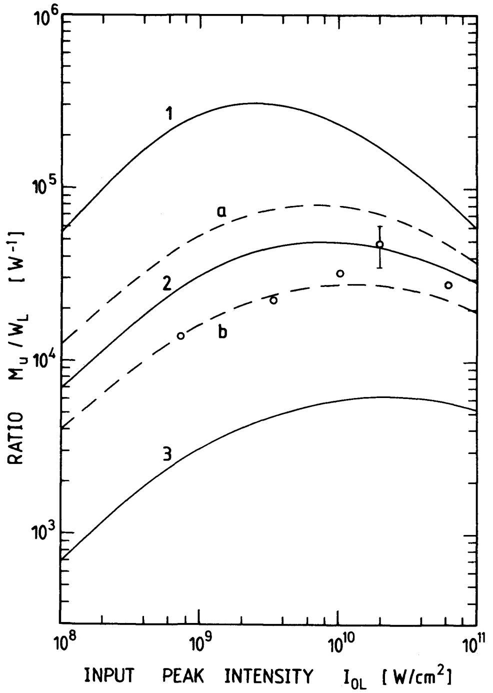

Figure 8 Normalized time integrated upper fluorescence level population M_4/W_L of dye 9740. Experimental points are derived from Equation 35. Solid curves: $\sigma_{ex} = 3.5 \times 10^{-17}$ cm^2, and 1, $\tau_F = k_{43}^{-1} = 10^{-12}$ s; 2, $\tau_F = 10^{-13}$ s; 3, $\tau_F = 10^{-14}$ s. Dashed curves: $\tau_F = 10^{-13}$ s, and a, $\sigma_{ex} = 1.75 \times 10^{-17}$ cm^2; b, $\sigma_{ex} = 7 \times 10^{-17}$ cm^2.

is positive and close to 0. This fact indicates an angle between the S_1–S_4 and the S_4–S_0 transition dipole moments of about $\alpha \simeq 50°$ (application of Equations 8, 9 or 13, 14). The S_1–S_0 fluorescence of rhodamine 6 G in ethanol is completely depolarized (Equation 18) since the reorientation time τ_{or} is short compared with the fluorescence lifetime.

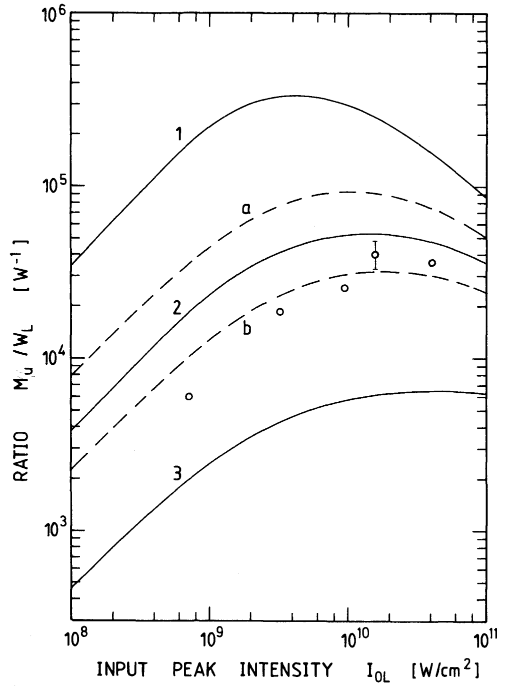

Figure 9 Normalized time integrated upper fluorescence level population M_4/W_L of dye 9860. Solid curves: $\sigma_{ex} = 2.5 \times 10^{-17}$ cm^2, and 1, $\tau_F = 10^{-12}$ s; 2, $\tau_F = 10^{-13}$ s; 3, $\tau_F = 10^{-14}$ s. Dashed curves: $\tau_F = 10^{-13}$ s, and a, $\sigma_{ex} = 1.25 \times 10^{-17}$ cm^2; b, $\sigma_{ex} = 5 \times 10^{-17}$ cm^2.

4. Conclusions

In the theoretical analysis formulae are derived that allow the determination of S_n-state lifetimes by S_n–S_0 fluorescence yield measurement after single pulse or double pulse two-step excitation. In the experimental section the S_4-state lifetimes of three mode-locking dyes for Nd-glass lasers are determined by single pulse two-step excitation. The upper fluorescence level population is determined by bleaching experiments where the excited state absorption cross-section is measured.

The S_n-state lifetime measurement by double pulse two-step excitation leads to a simple mathematical expression (Equation 36a) that needs no numerical calculations. The upper fluorescence level population is found directly by energy transmission measurements. The S_n–S_0 fluorescence signal initiated by one individual pump pulse has to be subtracted from the total double pulse fluorescence signal in the analysis [7, 10, 34].

The S_1–S_0 fluorescence of impurities hinders direct single-step S_n–S_0 fluorescence excitation [3]. In the two-step excitation process S_1–S_0 impurity fluorescence can only be excited by two-photon absorption. An analysis of the two-photon excited S_1–S_0 impurity fluorescence was carried out that allows an estimation of its importance to be made and makes it possible to discriminate between it and the S_n–S_0 fluorescence.

References

1. M. D. GALANIN and S. A. TSCHISCHKOWA, *Kratk. Soobschch. Fiz.* **4** (1971) 35.
2. J. L. RICHARDS and S. A. RICE, *Chem. Phys. Lett.* **9** (1971) 444.
3. G. ORNER and M. TOPP, *ibid.* **36** (1975) 295.
4. A. V. ARISTOV and V. S. SHEVANDIN, *Opt. Spectrosc.* **44** (1978) 276.
5. C. V. SHANK, E. P. IPPEN and O. TESCHKE, *Chem. Phys. Lett.* **45** (1977) 291.
6. V. L. BOGDANOV, V. P. KLOCHKOV and B. S. NEPORENT, *Opt. Spectrosc.* **43** (1977) 701.
7. I. KAPLAN and J. JORTNER, *J. Chem. Phys.* **32** (1978) 381.
8. W. FALKENSTEIN, A. PENZKOFER and W. KAISER, *Opt. Commun.* **27** (1978) 151.
9. A. PENZKOFER and W. KAISER, *Opt. Quantum Electron.* **10** (1978) 399.
10. M. R. TOPP, H. -B. LIN and K. -J. CHOI, *Chem. Phys.* **60** (1981) 47.
11. H. SCHÜLLER and H. PUELL, *Opt. Commun.* **3** (1971) 352.
12. C. LIN and A. DIENES, *ibid.* **9** (1973) 21.
13. J. R. HUBER and M. MAHANEY, *Chem. Phys. Lett.* **30** (1975) 410.
14. H. TASHIRO and T. YAJIMA, *ibid.* **42** (1976) 553.
15. R. W. ANDERSON, R. M. HOCHSTRASSER and H. J. POWNALL, *ibid.* **43** (1976) 224.
16. T. KOBAYASHI and S. NAGAKURA, *Chem. Phys.* **23** (1977) 153.
17. K. KASATANI, M. KAWASAKI and H. SATO, *ibid.* **83** (1984) 461.
18. M. MAHANEY and J. R. HUBER, *Chem. Phys. Lett.* **105** (1984) 395.
19. M. KASHA, *Disc. Faraday Soc.* **9** (1950) 14.
20. M. BEER and H. C. LONGUET-HIGGINS, *J. Chem. Phys.* **32** (1955) 1930.
21. M. MACIEJEWSKI and P. P. STEER, *Chem. Phys. Lett.* **100** (1983) 540.
22. C. A. PARKER, 'Photoluminescence of Solutions' (Elsevier, New York, 1968).
23. TH. FÖRSTER, 'Fluoreszenz Organischer Verbindungen' (Vandenhoeck und Ruprecht, Göttingen, 1951).
24. J. B. BIRKS, 'Photophysics of aromatic molecules' (Wiley Interscience, New York, 1970).
25. S. J. STRICKLER and R. A. BERG, *J. Chem. Phys.* **37** (1962) 814.
26. J. M. DEMAS and G. A. CROSBY, *J. Phys. Chem.* **75** (1971) 991.
27. A. PENZKOFER and W. BLAU, *Opt. Quantum Electron.* **15** (1983) 325.
28. P. M. RENTZEPIS, *Chem. Phys. Lett.* **2** (1968) 117.
29. B. NICKEL, *ibid.* **27** (1974) 84.
30. B. NICKEL and G. RODEN, *Ber. Bunsenges. Phys. Chem.* **81** (1977) 281.
31. H. B. LIN and M. R. TOPP, *Chem. Phys. Lett.* **47** (1977) 442.
32. H. B. LIN and M. R. TOPP, *ibid.* **48** (1977) 251.
33. M. R. TOPP and H. B. LIN, *ibid.* **50** (1977) 412.
34. H. B. LIN and M. R. TOPP, *ibid.* **67** (1979) 273.
35. B. I. STEPANOV and V. P. GRIBKOVSKII, 'Theory of Luminescence' (Iliffe, London, 1968).
36. P. P. FEOFILOV, 'The Physical Basis of Polarized Emission', (Consultants Bureau, New York, 1961).
37. E. D. CEHELNIK, K. D. MIELENZ and R. A. VELAPOLDI, *J. Res. Nat. Bur. Stand.* **79A** (1975) 1.
38. H. SATO, M. KAWASAKI and K. KASATANI, *Chem. Phys.* **83** (1984) 451.

39. A. YARIV, 'Quantum Electronics', 2nd Edn (Wiley, New York, 1975) p. 160.
40. J. B. BIRKS and D. J. DYSON, *Proc. Roy. Soc. London* **A275** (1963) 135.
41. F. GRAF and A. PENZKOFER, *Opt. Commun.* **51** (1984) 111.
42. A. PENZKOFER, D. VON DER LINDE and A. LAUBEREAU, *Opt. Commun.* **4** (1972) 377.
43. B. KOPAINSKY, W. KAISER and K. H. DREXHAGE, *ibid.* **32** (1980) 451.
44. D. VON DER LINDE and K. F. RODGERS, *IEEE J. Quantum Electron.* **QE-9** (1973) 960.
45. A. PENZKOFER, W. FALKENSTEIN and W. KAISER, *Chem. Phys. Lett.* **44** (1976) 82.
46. D. REISER and A. LAUBEREAU, *Appl. Phys.* **B27** (1982) 115.
47. A. V. ARISTOV and Yu. S. MASLYUKOV, *Opt. Spectrosc.* **41** (1976) 141.
48. T. J. CHUANG and K. B. EISENTHAL, *Chem. Phys. Lett.* **59** (1971) 368.